

Document downloaded from:

<http://hdl.handle.net/10251/149083>

This paper must be cited as:

Yamanaka, E.; Tortajada-Genaro, LA.; Maquieira, A. (2017). Low-cost genotyping method based on allele-specific recombinase polymerase amplification and colorimetric microarray detection. *Microchimica Acta*. 184(5):1453-1462. <https://doi.org/10.1007/s00604-017-2144-0>



The final publication is available at

<https://doi.org/10.1007/s00604-017-2144-0>

Copyright Springer-Verlag

Additional Information

Low-cost genotyping method based on allele-specific recombinase polymerase amplification and colorimetric microarray detection

Eric Seiti Yamanaka^(a), Luis A. Tortajada-Genaro^(a,b), Ángel Maquieira^(a,b)

(a) Instituto Inter-universitario de Reconocimiento Molecular y Desarrollo Tecnológico (IDM) - Departamento de Química, Universitat Politècnica de València, Camino de Vera s/n, E46022 Valencia, Spain

(b) Unidad Mixta UPV-La Fe, Nanomedicine and Sensors, Valencia, Spain

1 **ABSTRACT**

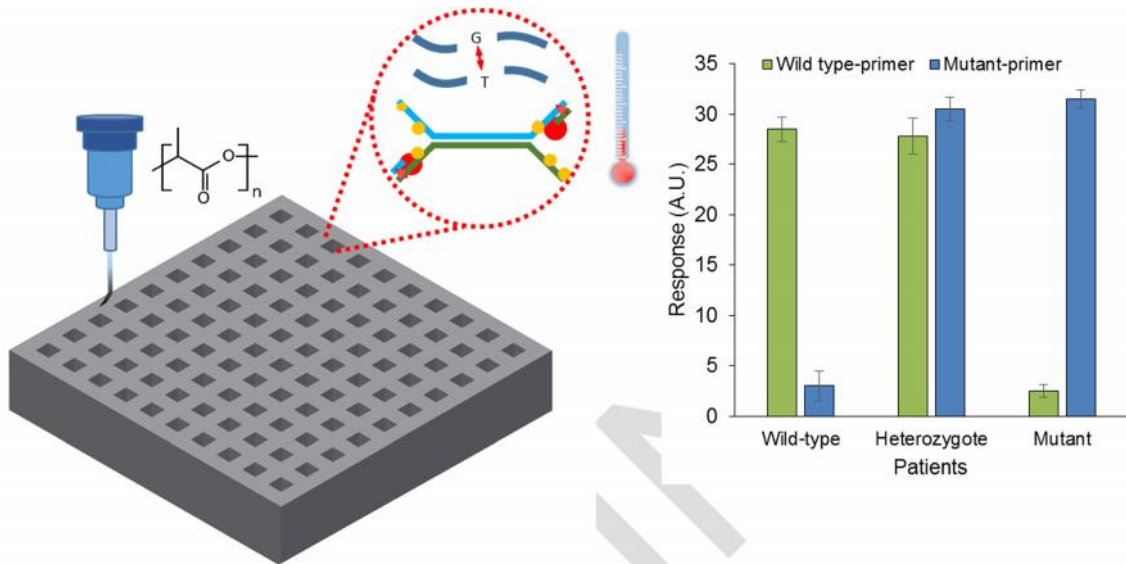
2 The costs of current genotyping methods limit their application to personalized
3 therapy. The authors describe an alternative approach for the detection of
4 single-point-polymorphisms (SNPs) using recombinase polymerase
5 amplification (RPA) as an allele-specific technique. The use of short and
6 chemically modified primers, locked nucleic acids (LNA), allowed the selective
7 isothermal amplification of wild-type or mutant variants at 37 °C in 40 min. An
8 amplification chip containing 100 wells was manufactured with a 3D printer and
9 using thermoplastic polylactic acid (PLA). The platform reduces costs, reagent
10 consumption, sample volume and allows assay parallelization compared to
11 other amplification formats. As proof of concept, the method was applied to the
12 genotyping of four SNPs that are related to the treatment of tobacco addiction.
13 The target polymorphisms were rs4680 (*COMT* gene), rs1799971 (*OPRM1*
14 gene), rs1800497 (*ANKK1* gene), and rs16969968 (*CHRNA5* gene). The
15 capabilities of the method are demonstrated detecting the reaction products
16 using a colorimetric technique in microarray format. The genotype populations
17 can be well discriminated.

18 Keywords: pharmacogenomics; SNP genotyping; isothermal amplification;
19 micro-well plate; microchip; tobacco addiction; 3D-printer; *COMT* gene; *OPRM1*
20 gene; *ANKK1* gene; *CHRNA5* gene.

ORIGINAL

21 **Graphical abstract**

22 A method based in the allele-specific recombinase polymerase amplification
23 was developed for the genotyping of polymorphisms. The isothermal
24 discrimination reaction was produced in a multi-well amplification chip
25 manufactured with a 3D printer and using thermoplastic polylactic acid.



26

27

28

ORIGINAL

29 INTRODUCTION

30 Pharmacogenomics is currently considered one of the most active areas of the
31 personalized medicine paradigm. However, numerous barriers have been
32 encountered to launch DNA variation analyses, such as single-nucleotide
33 polymorphisms (SNPs), in health systems [1]. Among other factors, available
34 platforms have a marked technological limitation. Most genomic findings have
35 been obtained from high-throughput technologies, such as Illumina and
36 Affimetrix platforms. However, the incorporation of these methods into primary
37 care centers is limited, and cost is the main drawback [2-4]. Dramatically cutting
38 the turnaround times of these platforms is an important goal for implementing
39 SNP testing into clinical scenarios. Therefore, the novel generation of simple
40 diagnostic tools is absolutely necessary for the real adoption of personalized
41 medicine [5,6].

42 A large family of high-potential methods to be developed in simple systems is
43 that based on allele-specific (AS) amplification [7]. Polymerase chain reaction
44 (PCR) uses primer pairs, deliberately designed at SNP sites. Primers have a
45 single-base variation at the 3' end (allele-specific primers), so extension and
46 amplification reactions take place with only perfectly-matched sequences of
47 target regions. This approach has been successfully used as a
48 pharmacogenomic tool combined with several detection systems [8-10].
49 Nevertheless, these techniques require particular thermal cycling, consequently
50 there are several limitations for their future integration as point-of-care devices.
51 PCR demands an accurate temperature control system to quickly heat/cool
52 reaction solutions. The high temperature reached (up to 95 °C) leads to
53 variations in the volume reaction due to water evaporation and gas bubble
54 formation, which renders accurate process control necessary.

55 Several new technologies have emerged to improve DNA-based analyses [11].
56 Many efforts have been made that focus on developing low-cost systems to be
57 used for point-of-care applications or in small laboratories located at the
58 physician's office or in primary health centers.

59 A revolution in the development of new methods is currently being witnessed,
60 and is associated with the application of isothermal solutions for microanalyses

61 [12]. These approaches are based on using proteins that separate DNA strands
62 instead of thermal approaches so that target nucleic acids are synthesized at
63 constant temperature. Nevertheless, the application of isothermal amplification
64 for SNP genotyping is still minimum [13,14]. Among isothermal reactions,
65 recombinase polymerase amplification (RPA) has many interesting properties;
66 e.g., short reaction times (20-60 min), robustness and low energy requirements
67 (close to room temperature) [15]. Recently, our research group has
68 demonstrated that polycarbonate-based substrates can be used to support RPA
69 assays in chip [16], micro-reactors [17], or dynamic formats [18]. A well array
70 chip has been described to process miniaturized RPA assays, applied for
71 pathogen detection in under 30 min [19]. The chip was manufactured from a
72 silicon substrate by a complex fabrication technique, including photolithography
73 and chemical treatment, and is only available in specialized laboratories.

74 The capability of RPA technology for SNP genotyping remains an unsolved
75 issue. A recent study evaluated the influence of sequence mismatches on the
76 amplification specificity of closely-related pathogens [20]. A proof of concept
77 assay describes the discrimination of a single-point mutation of the HRAS gene
78 [21]. To this end, DNA extracted from cell lines was selectively amplified and
79 genetic variants were distinguished by measuring the wavelength shift on silicon
80 micro-ring resonators. However, this technology is far from being adopted
81 generally in health centers.

82 In the present study, the capability of allele-specific RPA (AS-RPA) is evaluated
83 and a low-cost method is developed for the SNP genotyping of clinically
84 relevant polymorphisms. In a first approach, amplification is performed in
85 conventional polypropylene vials in a single format (detection of a single
86 polymorphism). The advantages of this disposable format are its low cost and
87 compatibility with a huge number of laboratory equipment. However, lab-on-a-
88 chip or μ -total analysis systems offer important advantages for diagnostic
89 devices, such as high-throughput and miniaturization, among others [22].

90 There are many ways to microfabricate plastic-based materials; e.g. laminate,
91 embossing or injection molding. Additive manufacturing is being examined
92 given its growing interest in the microfluidics field [23]. It is capable of producing

93 customized structures that range from a few microns to several centimeters in a
94 single step. The main limitations of 3D printers are related to spatial resolution,
95 dimensional fidelity, surface quality, biocompatibility, optical transparency,
96 among others [24]. Advantages include low infrastructure costs and easy
97 manufacturing compared to photolithography or soft lithography approaches. In
98 order to evaluate the potential of this technology, a well array chip for
99 performing AS-RPA was designed and developed with a commercial 3D printer.
100 The objective was to demonstrate RPA's capability as a genotyping method and
101 to compare its performance in an advanced platform compared to the standard
102 format (vials).

103 As proof of concept, the solution was applied as a pharmacogenomics tool to
104 treat smoking cessation and the highly addictive properties of nicotine [25,26].
105 In such diseases, the benefits of personalized medicine based on genotype
106 populations has been demonstrated. However, the high cost of current
107 genotyping technologies, compared to the cost of ineffective or erroneous
108 treatment, compromises the application of the test. Therefore, the approach
109 was designed by following the analytical quality and health system sustainability
110 goals.

111

112 **MATERIAL AND METHODS**

113 **Target genes**

114 The target polymorphisms for the tobacco use disorder were rs4680 (*COMT*
115 gene), rs1799971 (*OPRM1* gene), rs1800497 (*ANKK1* gene) and rs16969968
116 (*CHRNA5* gene). The wild-type variants are G, A, G, and G, and the mutant
117 variants are A, G, A, and A, respectively. The pharmacogenomic information
118 about these variants is included as Supplementary Material (Tables SI.1, SI.2
119 and SI.3). The human beta actin (*ACTB*) gene was selected as an endogenous
120 control. The list of oligonucleotides for the genotyping of each SNP is found in
121 Table SI.4.

122

123

124 **Patient samples and reference discrimination method**

125 Subjects (n=17) were recruited for the present study according to ethics and
126 with informed consents. Buccal smear samples were collected using sterile
127 swabs. They were submitted to digestion and purification steps with a PureLink
128 Genomic DNA Mini Kit (Invitrogen, Thermo Fisher Scientific, USA,
129 www.thermofisher.com). The isolated DNA extracts were eluted from the spin-
130 columns of the kit with Tris-HCl buffer (10 mM Tris, pH 8.6) and stored at -20 °C
131 until analyzed.

132 Allele-specific PCR in a single format was applied as the reference genotyping
133 method. Briefly, the extracted genomic DNA (4 ng) was amplified using two
134 PCR master mixes (Biotools, Spain, www.biotools.eu) and employing 300 nM of
135 each variant primer pair (reverse and allele-specific forward). To confirm
136 amplification, products were diluted in 0.5x SyBR Safe (Invitrogen, Thermo
137 Fisher Scientific, USA) and submitted to fluorescence measurements in a plate
138 reader (Victor 3™ V1420, PerkinElmer, Finland, www.perkinelmer.com).
139 Genotypes were also verified by 3% agarose gel electrophoresis, followed by
140 dyeing with an intercalating agent (Real Safe, Durviz, Spain, www.durviz.com)
141 and visualization under UV light.

142

143 **Fabrication of structured platforms**

144 The 100-well array chip was modeled with the Autodesk Inventor Professional
145 2015 software (Autodesk, USA, www.autodesk.com) and fabricated with a 3D
146 printer (Ultimaker 2 Extended, Ultimaker B.V., the Netherlands,
147 www.ultimaker.com). Polylactic acid (PLA) filament (RS Pro, Spain; 2.85 mm
148 diameter, www.rs-online.com) was employed as the printing material.
149 Fabrication was carried out using a 0.4 mm diameter nozzle at 210 °C and a
150 bed operation temperature of 60 °C. In order to evaluate the best printing
151 conditions, prototypes were fabricated with different layer thicknesses (up to 0.2
152 mm) and at various printing speeds (up to 300 mm·s⁻¹). Subsequently, printed

153 structures were cleaned with a 30-minute ultrasonic bath and dried with
154 compressed air.

155 The fabrication quality of the PLA-chips was monitored by optical microscopy
156 imaging. Surface pictures were captured (1.2x magnification) by an Olympus
157 SZ61 stereo microscope (Olympus Co., Japan, www.olympus.com). Images
158 were analyzed with the Image J software to provide an estimated roughness for
159 each sample. Surface hydrophobicity was estimated from the contact angle
160 data. Measures of the deionized water droplets (4 μ L) were taken using a Dino-
161 Lite Digital Microscope (AnMo Electronics Co., Taiwan, www.dino-lite.com) at
162 the 1.3 megapixel resolution.

163 A mass loss study was also done to evaluate possible sample evaporation on
164 the platform. The chip was loaded with 10 RPA samples (4 μ L each) and placed
165 in an oven at 37 °C. Mass measurements of the set were periodically taken
166 during 4 h and compared with those of an unloaded reference chip.

167

168 **Assay protocol: amplification**

169 The amplification step was performed using a TwistAmp Basic RPA kit
170 (TwistDx, UK, www.twistdx.co.uk). Eight allele-specific mixes (2 per SNP) were
171 prepared with rehydration buffer, 14 mM of magnesium acetate, 480 nM of
172 allele-specific forward primer and reverse digoxigenin-labeled primer, and the
173 enzyme pellet. Mineral oil (8%) was also added to minimize sample
174 evaporation. Solutions were loaded onto the 100-well array chip and the DNA
175 template (2.56 ng) was added to allow the simultaneous amplification of eight
176 different allelic variants for 10 patient samples and controls (human *ACTB*
177 gene). The chip was then covered with a polyester plate sealer (Corning, USA,
178 www.corning.com) and gently vortexed to mix reagents and samples.
179 Amplification was carried out in a heating oven (Mettler UF30, Germany,
180 www.mettler.com) at 37 °C for 40 min.

181 The AS-RPA reactions were also performed in 0.2 mL-polypropylene vials
182 (Labbox, Spain, www.labbox.com) and polycarbonate home-made array chips.
183 These chips were fabricated using a computer numerical control drilling

184 machine (Bungard CCD, Karo 5410, Germany, www.bungard.de). The feed
185 speed and rotational rate of the drill were respectively 2 000 mm·s⁻¹ and 48 000
186 rpm. The diameter of each well was 5 mm and their depth was 1.1 mm. The
187 composition of the RPA mixtures was the same as that previously described,
188 but volumes were 25 µL and 4 µL per reaction for vials and chips, respectively.
189 The heating system used was a thermocycler (TC-4000, Techne, UK,
190 www.techne.com) and an oven, respectively.

191

192 **Assay protocol: detection and data analysis**

193 The AS-RPA products were detected by a hybridization assay on polycarbonate
194 chips, adapted from reference [10]. Briefly, the mixtures of the wild-type or
195 mutant products for all four SNPs were prepared from the respective single
196 RPA solutions. For this purpose, 2 µL of each amplification product were diluted
197 in 16 µL of hybridization buffer composed of NaCl 225 mM, sodium citrate 22.5
198 mM, 10% formamide and 2.5x Denhardt's solution, pH 7. Subsequently,
199 mixtures were heated at 95 °C for 10 min for denaturation and transferred to the
200 chips with the immobilized probes in the microarray format. After 60 min of
201 incubation at 37 °C, chips were washed with diluted hybridization buffer. The
202 immunoreaction protocol with enzymatic labelling was followed to develop the
203 duplex of the probe-RPA product, as described in reference [10]. The oxidized
204 form of 3,3',5,5'-tetramethylbenzidine (substrate of horse-radish-peroxidase)
205 produced a blue precipitate over the positive or control spots. Chips were then
206 read with a desktop scanner (Epson Perfection 1640SU Office, Epson, Japan,
207 www.epson.com).

208

209 **Discrimination index**

210 The resulting gray-scale images (Tagged Image File Format, color depth 16 bit)
211 were processed by an in-house software for the microarray analysis. The optical
212 intensity signals of each spot and local background were quantified by
213 generating a data matrix of the signal-to-noise ratios. The genotype
214 determination rule was constructed according to the replicated responses of the

215 specific probes for each polymorphism. A discrimination index was calculated
216 from the signal of the wild-type (WT) and mutant (MUT) variants according to
217 this equation: $(WT - MUT)/(WT + MUT)$. The Statgraphics Centurion statistical
218 package for Windows v.16 was used for the data analysis.

219

220 **RESULTS**

221 **RPA capability as a genotyping tool**

222 The use of RPA as an allele-specific amplification technique was analyzed by
223 considering the role of each element in the process. A recombinase (T4 uvsX)
224 recognizes targeted DNA templates and specific primers at a high affinity and
225 catalyzes subsequent homologous pairing and strand exchange [20].
226 Polymerase produces the correct elongation of the perfect-annealed
227 primer/template, and is the key reaction in the DNA duplication process [27].
228 Furthermore, the Pol I large fragment (Bsu polymerase) lacks exonuclease
229 activity (3'→5') that may modify the target nucleotide. Therefore, we expected
230 the presence of mismatches on their 3'-extreme to hamper the nonspecific
231 reaction due to the combined action of two enzymes, even at a low working
232 temperature.

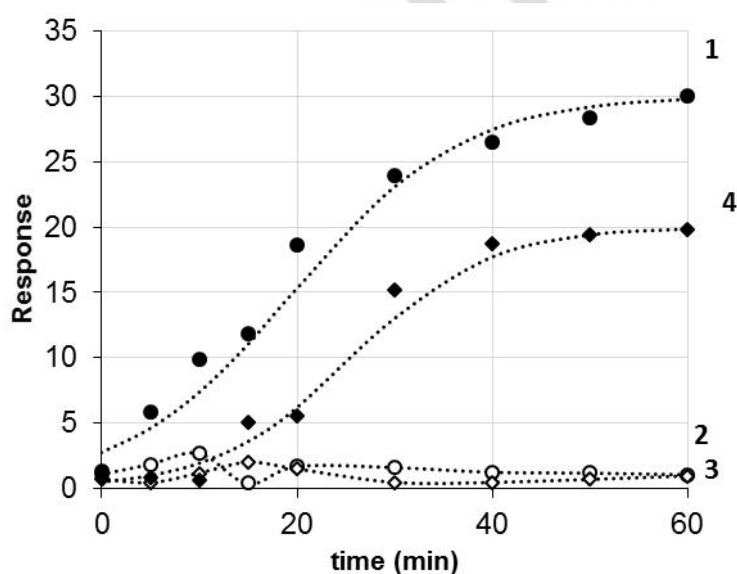
233 Complementarily, oligonucleotide sets were carefully selected to satisfactorily
234 amplify/detect the given template region. The *in silico* design restrictions were
235 primer length, absence of secondary structures, and primer/template duplex
236 stability. Both these last parameters were estimated from the thermodynamic
237 models available for DNA duplexes [28]. Although the recommended length for
238 RPA primers should be 30-35 bases long according to the manufacturer's
239 instructions, shorter primers (19–21 mer) were chosen to improve selectivity.
240 The free energy (ΔG) values for the self-annealing and hairpin structures were
241 restricted to 1.0 Kcal·mol⁻¹ (the equivalent to melting temperatures < 50 °C).
242 The selected oligonucleotides produced primer/template duplexes with changes
243 in free energy (ΔG) of -25.6 ± 0.2 Kcal·mol⁻¹ (the equivalent to a melting
244 temperature of 75.4 ± 0.1 °C) for totally complementary primers. The duplexes

245 between the template and mismatched primers were less stable (-24.0 ± 0.6
246 $\text{Kcal} \cdot \text{mol}^{-1}$, 72.7 ± 0.6 °C).

247 The experiments focused on evaluating discrimination capability using the
248 designed primers that differentiated at their 3'-endnucleotide. Figure 1a shows
249 the kinetic curve to perform amplification in a homogeneous format (reaction
250 volume of 25 μL). The expected positive signals were observed after 10-20 min
251 following typical logistic regression (maximum response after 60 min). Under
252 the selected conditions, a different behavior was observed depending on the
253 added primer. Extension by polymerase was efficient when the 3' terminal base
254 of a primer matched its target, whereas extension was inefficient or nonexistent
255 when the terminal base was mismatched. These effects agree with the
256 previously reported results about the reduction or inhibition of the RPA reaction
257 due to the presence of a mismatch in the primer/template duplex [20].

258

(a)

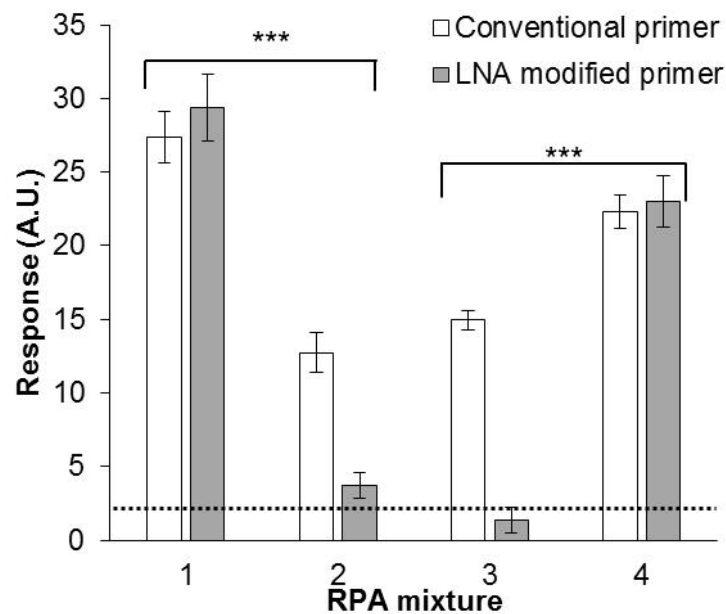


259

260

261

(b)



262

263 **Figure 1.** (a) Amplification kinetic curves of rs1799971 (*OPRM1* gene)
 264 depending on the RPA mixture: logistic regressions $y = 30 / (1 + \exp(-2.28 - 0.12$
 265 $t))$, $R = 0.977$ for the wild-type and $y = 20 / (1 + \exp(-3.64 - 0.15 t))$, $R = 0.977$ for
 266 the mutant variant. (b) Response depending on the primer nature and RPA
 267 mixture: statistical comparison compared to the perfect-match duplex (**
 268 $p < 0.001$). Mixture 1: wild-type template DNA and wild-type FP). Mixture 2: wild-
 269 type template DNA and mutant FP. Mixture 3: mutant template DNA and wild-
 270 type FP. Mixture 4: mutant template DNA and mutant FP. Four replicates

271

272 Conventional and chemical-modified primers, locked nucleic acids (LNA), were
 273 compared for AS-RPA. Figure 1b shows that nonspecific amplification took
 274 place for the mismatched duplexes between the primer and templates.
 275 Nevertheless, the amplification yield was significantly higher for the totally
 276 complementary duplexes (ANOVA, p -value < 0.001). With the LNA primers,
 277 differences were more marked, and even nonspecific amplification was similar
 278 to the negative controls. These experiments demonstrated that the presence of
 279 this nucleoside at the 3' terminal base improved allelic discrimination.

280 A multiplex reaction was studied for the simultaneous amplification of more than
 281 one target in a single reaction. However, reaction yields were not satisfactory
 282 and there were sensitivity losses. One system displayed dominating and/or

283 inhibiting activity over other primers and amplicons, and even genotyping
284 capability was lost. These results agreed with conventional RPA behavior and
285 can be associated with their high sensitivity to the total primer concentration
286 [16].

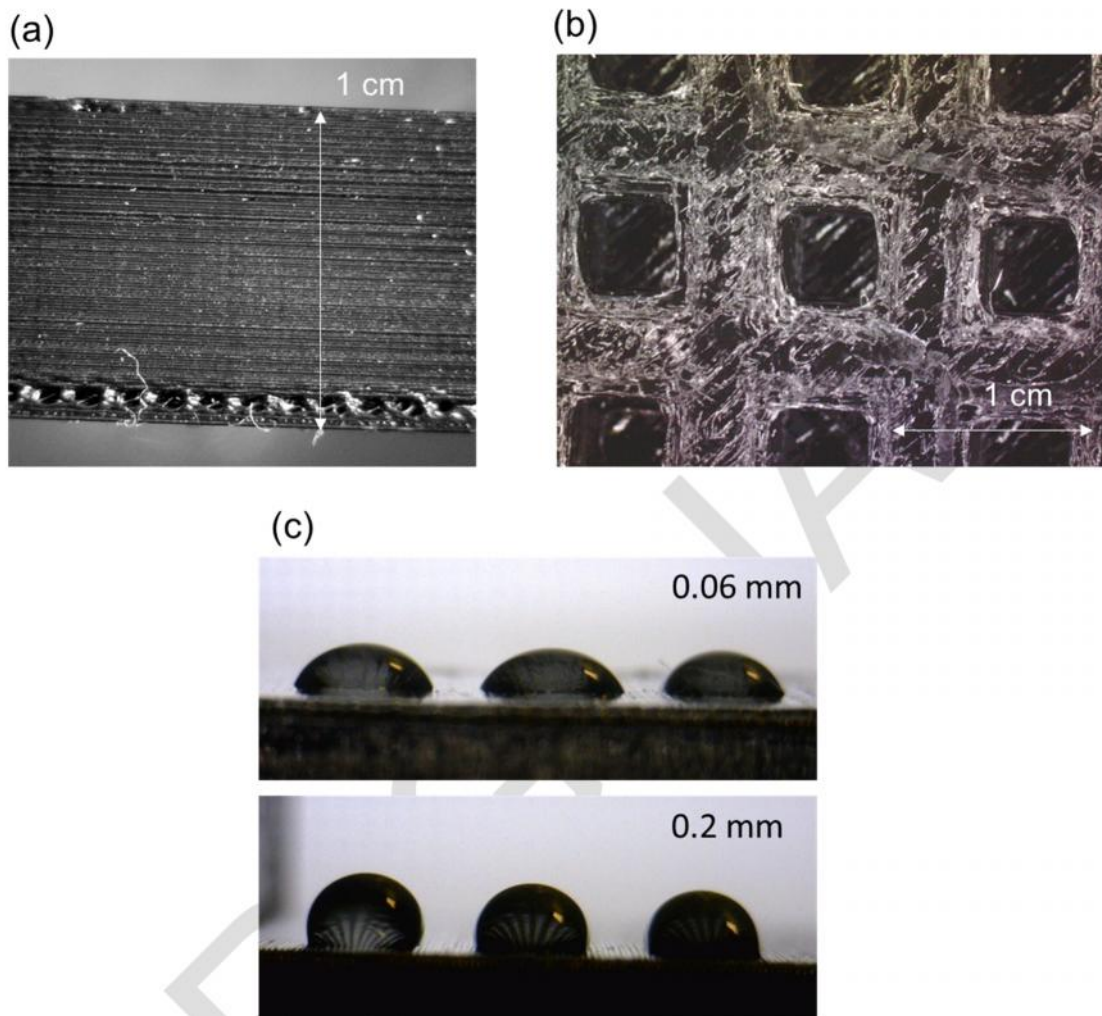
287

288 **Design and fabrication of well array chip**

289 The amplification assays, described in the previous section, were performed in
290 0.2-mL polypropylene vials. The next step was to reduce the reaction volume by
291 performing the assay in a well array chip. This kind of platforms improves
292 amplification capabilities, particularly high-throughput [29]. Fused filament
293 fabrication was chosen as the additive manufacturing technology, with a
294 biocompatible polymer, e.g., PLA, as the thermoplastic material. This technique
295 was selected because it produces innovative bioanalytical platforms that can be
296 customer-designed and fast prototyped by a 3D printer.

297 The first experiments focused on designing an array chip with 100 wells. The
298 well dimensions (2.5 mm × 2.5 mm × 4 mm) were chosen to perform RPA in a
299 reduced volume (<5 μ L). Edge-to-edge spacing (distance between wells) was 1
300 cm for RPA-mixture dispensation by a multi-channel micropipette. The
301 deposition of filament layers, one on top of the other, built up the bottom and the
302 walls of the chip. This additive technique produced grooved structured surfaces
303 on chip walls to study the effect of the 3D printing parameters on chip quality
304 (Supplementary Material/Figure SI.1). By increasing printing layer separation,
305 groove thickness changed from 71 \pm 2 μ m (0.06 mm) to 238 \pm 5 μ m (0.2 mm).
306 With a 0.02-mm layer height, the surface became irregular and did not produce
307 visible grooves. Surface roughness, expressed in Rq, varied from 53.8 μ m (0.02
308 mm) to 76.6 μ m (0.2 mm). The effect of printing speed and working
309 temperatures during the deposition process were negligible. The selected
310 values were a layer height of 0.1 mm and a print speed of 50 mm·s⁻¹, which
311 resulted in a fabrication time of 480 min·unit⁻¹. Figures 2a and 2b show the
312 optical microscope images of the PLA-chips produced under the selected
313 conditions. Sealing, performed with a polyester adhesive film and by adding

314 mineral oil, was effective for the tested range (up to 37 °C and 4 h), with null
315 leaking and evaporation (p-value < 0.001).



316

317 **Figure 2.** (a) Optical microscope image of the chip wall. (b) Optical microscope
318 image of chip wells (top view). (c) Effect of printing layer height on the PLA
319 contact angle

320

321 The hydrophilic/hydrophobic nature of the reaction vessel can affect the easy-
322 filling of wells. Hence the wettability of the raw PLA-chips was estimated and
323 the contact angle of well surfaces was measured. The results were $97 \pm 4^\circ$ and
324 $77 \pm 2^\circ$ for the wall and the bottom surface, respectively. These values indicated
325 how the patterned topography modified the interfacial tension between the liquid
326 and thermoplastic compared to the base material (PLA, contact angle of about
327 80°). Two chemically modified chips (UV/ozone irradiation and PEG

328 passivation) were tested. The surface topographies, estimated by microscope
329 image analyses, were comparable to those from the raw chip (p-value > 0.05).
330 After applying soft UV/ozone irradiation, the contact angle was $71\pm 2^\circ$. This
331 lower value indicated that some photo-oxidized polar groups on the surface
332 were formed, consequently fiber adhesion increased (higher surface energy).
333 Addition of PEG also produced a coating over all the active surfaces, and
334 hydrophilicity increased ($62\pm 3^\circ$). Regardless of the surface treatment, reagent
335 solutions were easily loaded in wells.

336 The effect of the unpolished surfaces and chemical treatment on the
337 amplification yield was studied. Replicate RPA reactions were performed using
338 genomic DNA for native/mutant patients (order of magnitude: 10^3 pg of gDNA).
339 Effective amplification was achieved in all the wells of the raw and chemically
340 modified PLA-chips. Nevertheless, the PEG coating was chosen because this
341 treatment can help block chip surfaces, and prevent nonspecific signals and
342 sample losses through protein and amplification product adsorption [30].

343

344 **Comparison of amplification platforms**

345 The RPA performances for the reactions run in the PLA-3D printed chip were
346 compared with two previously reported platforms (Table 1). The first reference
347 platform was polypropylene vials (0.2 mL) (individual or tube strips), which are
348 widely used for DNA amplification in conventional thermal cyclers. The second
349 was micro-reactors fabricated in polycarbonate (PC) substrate by drilling
350 because they are a low-cost alternative for reduced volume amplifications
351 performed in ovens or other cheap thermal systems [17]. The analysis of
352 variance (ANOVA) indicated that the responses for three platforms were
353 comparable, with p-values of 0.63 for the negative controls, 0.27 for the
354 reference gene (*ACTB* gene) and 0.23 for the target genes. The platform cost
355 for 100-plex reactions using the current 3D-printed chips was the equivalent to
356 those of the polypropylene vials. Nevertheless, the main advantages of this
357 approach stemmed from volume reduction and the cost of the reagent; reagent
358 consumption (and the amount of DNA) decreased by about 6-fold. Other
359 advantages were reduced size, which was compatible with portable heating

360 systems (i.e. miniaturized Peltier-based devices), and facilitated their adaptation
361 for field or doctor office applications [11,12]. These performances confirmed
362 PLA-additive manufacturing to be a strategy for the rapid versatile low-cost
363 prototyping of bioanalytical devices. The assay costs of each platform were
364 estimated, considering their material, equipment and processing expenses (3D
365 printing or CNC milling), as well as their number of parallel assays. The
366 estimated platform cost per assay for the 3D printed PLA chip was similar to
367 polystyrene vials, while 4-times lower than for the polycarbonate milled chips.

368 Our approach based on reaction vessels was compared with microfluidic chips
369 in virtue of their high applicability as point-of-care systems [31]. The microfluidic
370 platforms, generally based on poly(methyl-methacrylate) (PMMA) or similar
371 polymers, allow a higher degree of assay integration and lower reaction
372 volumes (nanoliter scale). In exchange, the PLA multi-well chip presents easier
373 manipulation, no fluidic control equipment requirements and a simpler
374 fabrication process with a 16-fold lower cost.

375 This study can open up ways to test PLA-microfluidic devices, e.g., integration
376 of RPA amplification and real-time detection, prior to their mass production in
377 other thermoplastics, such as PC (e.g., injection molding).

378

379

380

381

382

383

384




385

386

387

388

389 **Table 1.** Characteristics of the tested amplification platforms

| |  |  |  |
|--------------------------------|-----------------------------------------------------------------------------------|-----------------------------------------------------------------------------------|-------------------------------------------------------------------------------------|
| | PLA chip | PP vial | PC chip |
| Response negative control | 3 ± 2 a.u. | 4 ± 1 a.u. | 4 ± 1 a.u. |
| Response reference gene | 37 ± 3 a.u. | 41 ± 2 a.u. | 39 ± 3 a.u. |
| Response target genes | 34 ± 3 a.u. | 37 ± 1 a.u. | 35 ± 1 a.u. |
| Fabrication technique | 3D printing | Molding | Molding + Milling |
| Platform dimensions | 52 mm × 52 mm × 10 mm | 100 × (20 mm, φ 7 mm) | 30 mm × 30 mm × 12 mm |
| Material thermal conductivity | 0.13 W·m ⁻¹ ·K ⁻¹ | 0.20 W·m ⁻¹ ·K ⁻¹ | 0.19 W·m ⁻¹ ·K ⁻¹ |
| Number of simultaneous samples | 100 | 1 | 9 |
| Reaction volume per assay | 4 μL | 25 μL | 4 μL |
| DNA amount per assay | 2.56 ng | 16 ng | 2.56 ng |

390 a.u.: arbitrary units. Data from three replicated assays

391

392 Analytical performance of the genotyping assay

393 Having demonstrated that AS-RPA can be used for SNP genotyping in a single
 394 format, the capabilities of a multiplex detection method were studied. Among
 395 the techniques currently available (i.e. optical, electrochemical, etc.), AS-RPA
 396 on PLA chips combined to a hybridization assay on PC chips was tested. This
 397 detection approach showed excellent performance to simultaneously identify
 398 several PCR products [10].

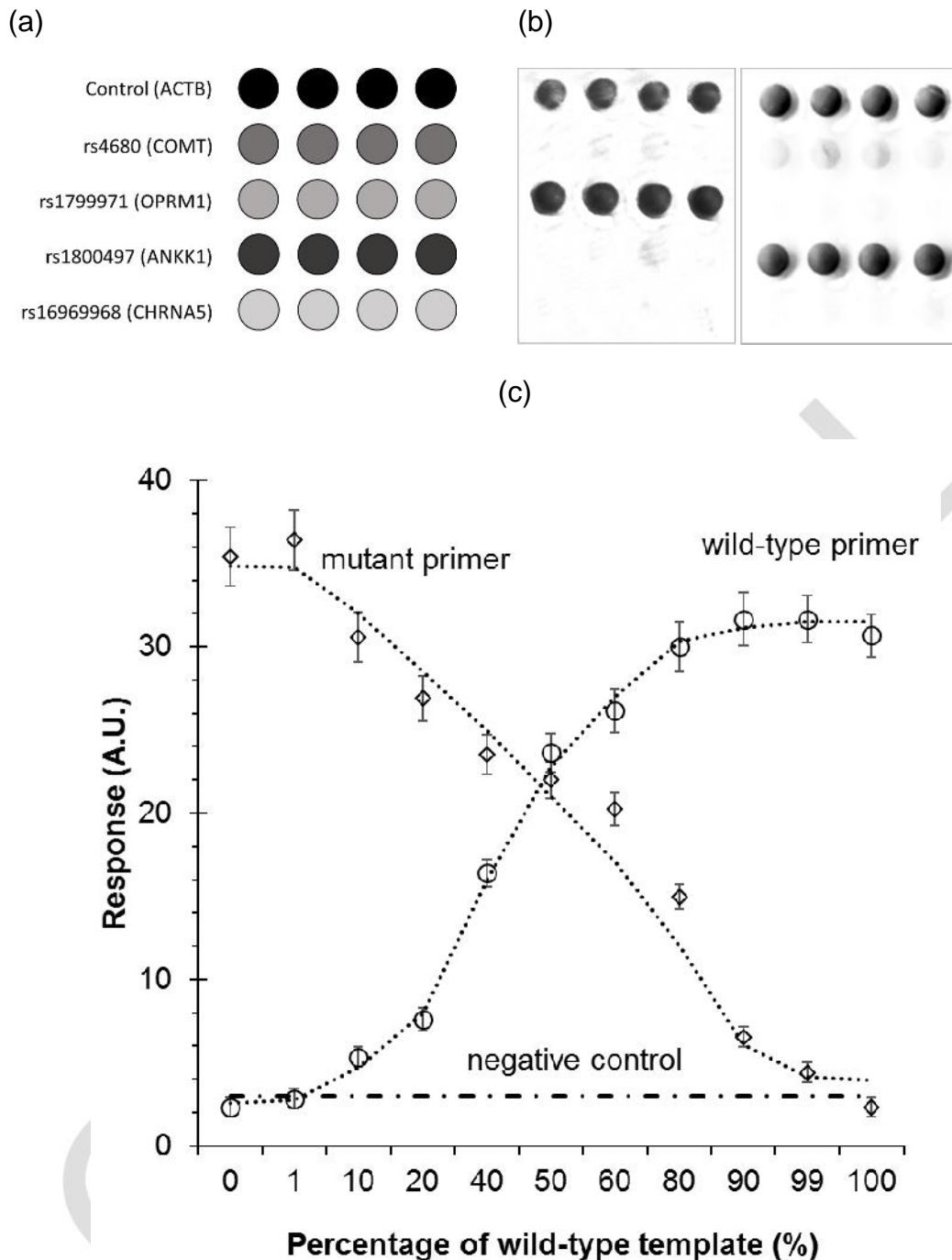
399 The AS-RPA products from the target genes related to the tobacco use disorder
 400 were simultaneously determined. Selectivity was estimated from cross-reactivity
 401 experiments by hybridizing products from single amplification assays on a chip
 402 that contained probes for the five studied genes (four target genes and a control
 403 gene) (Figure 3). Positive responses were obtained only for the specific probe,
 404 and were negative for the remaining ones. Sensitivity was determined by
 405 preparing heterozygous mixtures with increasing percentages of wild-type DNA

406 compared to the mutant type (Supplementary Material). Mismatched DNA was
407 detected up to 5-10 %, which indicated that the system was capable of
408 discriminating both genotypes selectively. Intra-day repeatability and inter-day
409 reproducibility, expressed as the relative standard deviation of spot intensities
410 for the replicated assays (five replicates), were 13 % and 17 %, respectively.
411 The ANOVA test showed that the end-point responses were comparable for the
412 four studied genes (p-value > 0.05).

413 Our detection method of AS-RPA products displayed comparable performance
414 to others previously described for AS-PCR, such as capillary electrophoresis
415 [8], real-time fluorescence [32], the fluorescent-based droplet technique [9] and
416 hybridization to covalently immobilized probes in fluorescent magnetic beads
417 [33].

418

ORIGINAL MANUSCRIPT



419

420 **Figure 3.** (a) Probe layout of a microarray chip (b) Microarray images obtained
 421 for the amplification products: rs1799971 (left) and rs1800497 (right).(c) Assay
 422 response depending on the percentage of wild-type template compared to the
 423 total template for both RPA mixtures (wild-type FP and mutant FP). Logistic
 424 regressions: $y = 32 / (1 + \exp(2.43 - 0.07 t))$, $R = 0.982$ for the wild-type and $y =$
 425 $37 / (1 + \exp(-2.80 + 0.05 t))$, $R = -0.935$ for the mutant.

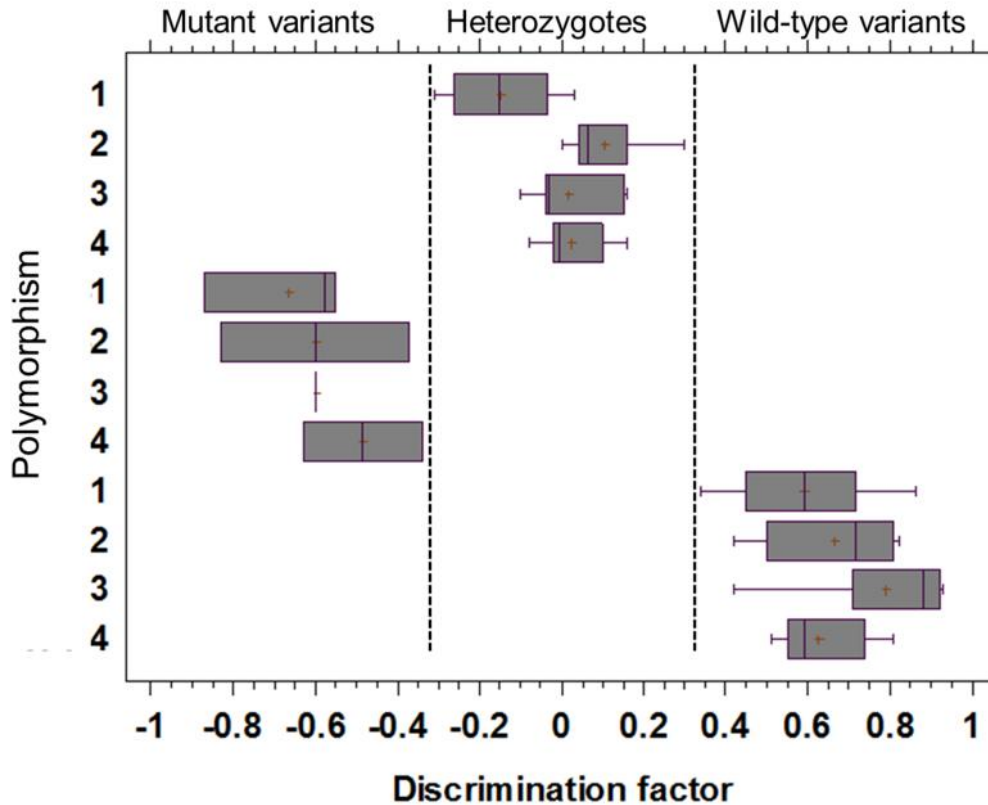
426 **Analysis of patient samples**

427 The applicability of chip-based AS-RPA for genotyping screening in tobacco
428 cessation treatment, or for drugs used in nicotine dependence, was
429 investigated. As a biological sample, buccal swab extracts were selected. In a
430 clinical scenario, the use of buccal swabs is noninvasive, less stressful and a
431 much easier technique to collect DNA samples. Moreover, sample storage does
432 not require refrigeration and DNA extraction is a much simpler process than
433 blood samples. As a detection strategy, a desktop scanner was used for chip
434 reading. Then the procedure was performed using low-resource laboratory
435 materials and equipment (i.e. a primary health center). The analysis time was
436 210 min (DNA extraction: 50 min, amplification: 60 min, hybridization-detection:
437 100 min).

438 The absorption measurements indicated that a sufficient amount of high quality
439 amplifiable human DNA was isolated from all the tested samples. The reference
440 (*ACTB* gene) and targeted regions were amplified and submitted to on-chip
441 hybridization. Figure SI.3 illustrates some examples of the microarray images.
442 Presence of mutated variants in rs4680 and rs1799971 was detected. A
443 subsequent comparison of the acquired chip signals with patient stratification
444 based on the reference method clearly demonstrated perfect matching. The
445 clinical implications of the provided genotyping results are a review of drug
446 treatment, including anti-depressives or nicotine replacement products (e.g.
447 patch). Functional polymorphisms in dopamine pathways (rs4680) are
448 associated with the use of bupropion to mitigate lapsing to smoking following a
449 quit attempt [34]. Better prolonged abstinence rates have been reported after
450 the nicotine replacement therapy tailored to each smoker, and based on either
451 genotype in the opioid receptor (rs1799971) [26].

452 Presence of mutant alleles was detected for 70.6 % (rs4680), 52.9 %
453 (rs1799971), 41.2 % (rs1800497), and 41.2 % (rs16969968) of the smoker
454 patients. A discrimination factor for genotype assignment was calculated from
455 the signal-to-noise ratios recorded in the microarray images (Figure 4). Each
456 call type within each target polymorphism statistically and significantly differed
457 from the others (p-values <0.0001). Homozygous genotypes led to

458 discrimination factors above 0.3 and under -0.3 for the wild-type and the
459 mutant, respectively. An intermediate discrimination factor (between -0.3 and
460 $+0.3$) was calculated for each heterozygous genotype. The genotype
461 assignments, listed in Supplementary Material, agreed with those obtained by
462 the reference method (100 % coincidence).



463

464 **Figure 4.** Boxplots of the discrimination factors classified according to the
465 polymorphism and population group. 1: rs4680, 2: rs1799971, 3: rs1800497,
466 and 4: rs16969968

467

468 CONCLUSIONS

469 In the last few decades, patient genome information has been proposed to
470 select individual clinical care, particularly drug treatment decisions. However,
471 the impact of personalized medicine is low compared to the research advances
472 made. The results reported herein study demonstrate how pharmacogenomics
473 knowledge combined with emerging analytical methodologies can benefit
474 clinical practice more broadly. Although more in-depth research must be

475 conducted, the combination of two innovative solutions was a success. Firstly,
476 the advantages of the isothermal amplification reaction were incorporated to
477 acquire the demanded copy number for sensitive SNP loci detection. The best
478 features were their fast-response (4-fold compared to the PCR), low
479 temperature (37 °C) and few design restrictions. However, the reduced
480 multiplexing capabilities forced single parallelized reactions. Secondly, we
481 employed additive manufacturing based on using a 3D printer as the chosen
482 technology to create a customer-tailored platform for high-throughput analyses.
483 The 100-well PLA-chip design considerably reduced reagent consumption and
484 avoided expensive manufacturing processes or complex pumping systems
485 associated with some DNA detection instruments. In fact the assay can be
486 performed with standard materials (i.e. pipettes, oven) found in clinical
487 laboratories. The present work demonstrates that PLA is an adequate material
488 for performing enzymatic reactions in a static format. The following step is to
489 achieve better point-of-care performance and the next challenge is to develop
490 microfluidic devices fabricated with this material that integrate all DNA assay
491 steps, from extraction to detection. The advantages include the method's
492 flexibility and accessibility compared to other micro-prototyping or micro-
493 fabrication techniques.

494 Regarding the clinical impact, today pharmacogenomics is applied mainly to
495 certain treatments in psychiatry, oncology and cardiology. One main reason is
496 the cost-effectiveness of genotyping methods. In addition, only some diseases
497 apply to this approach because their treatment generally involves expensive
498 pharmaceutical products or drugs with highly probable adverse effects. With our
499 approach, personalized therapies based on incorporating genetics into patient
500 stratification can be offered, and even for relatively less-impact treatments. The
501 methodology's cost-effectiveness, flexibility and portability will support the well-
502 known genetic marker for predicting drug responses. In the particular case of
503 tobacco addiction, genotyping information will help predict the degree of
504 success in smoking cessation.

505

506 **Acknowledgements**

507 The authors acknowledge the financial support received from the Generalitat
508 Valenciana (GVA-PROMETEOII/2014/040 Project and GRISOLIA/2014/024
509 PhD grant) and the Spanish Ministry of Economy and Competitiveness
510 (MINECO CTQ2013-45875-R project).

511 REFERENCES

512 (1) Manolio TA, Chisholm RL, Ozenberger B, Roden DM, Williams MS,
513 Wilson R, *et al.* (2013) Implementing genomic medicine in the clinic: the future
514 is here. *Genet Med* 15:258-267.

515 (2) Scott SA (2013) Clinical pharmacogenomics: Opportunities and
516 challenges at point-of-care. *Clin Pharmacol Ther* 93:33.

517 (3) Limaye N (2013) Pharmacogenomics, Theranostics and Personalized
518 Medicine-the complexities of clinical trials: challenges in the developing world.
519 *Appl Transl Genomics* 2:17-21.

520 (4) Abul-Husn NS, Owusu Obeng A, Sanderson SC, Gottesman O, Scott SA
521 (2014) Implementation and utilization of genetic testing in personalized
522 medicine. *Pharmacogenomics Pers Med* 7:227-40.

523 (5) Knez K, Spasic D, Janssen KP, Lammertyn J (2014) Emerging
524 technologies for hybridization based single nucleotide polymorphism detection.
525 *Analyst* 139:353-370.

526 (6) Shen W, Tian Y, Ran T, Gao Z (2015) Genotyping and quantification
527 techniques for single-nucleotide polymorphisms. *TrAC Trends Anal Chem* 69:1-
528 13.

529 (7) Milbury CA, Li J, Makrigiorgos GM (2009) PCR-based methods for the
530 enrichment of minority alleles and mutations. *Clin Chem* 55:632-640.

531 (8) Asari M, Watanabe S, Matsubara K, Shiono H, Shimizu K. (2009) Single
532 nucleotide polymorphism genotyping by mini-primer allele-specific amplification
533 with universal reporter primers for identification of degraded DNA. *Anal*
534 *Biochem* 386:85-90.

535 (9) Taira C, Matsuda K, Yamaguchi A, Sueki A, Koeda H, Takagi F,
536 Kobayashi Y, Sugano M, Honda T. (2013) Novel high-speed droplet-allele
537 specific-polymerase chain reaction: Application in the rapid genotyping of single
538 nucleotide polymorphisms. *Clin Chim Acta*, 424:39-46.

539 (10) Tortajada-Genaro LA, Mena S, Niñoles R, Puigmule M, Viladevall L,
540 Maquieira A (2016) Genotyping of single nucleotide polymorphisms related to
541 attention-deficit hyperactivity disorder. *Anal Bioanal Chem* 408:2339-2345.

542 (11) Woolley CF, Hayes MA (2014) Emerging technologies for biomedical
543 analysis. *Analyst* 139:2277-2288.

544 (12) Craw P, Balachandran W (2012) Isothermal nucleic acid amplification
545 technologies for point-of-care diagnostics: a critical review. *Lab Chip*, 12:2469-
546 2486.

547 (13) Zhang L, Zhang Y, Wang C, Feng Q, Fan F, Zhang G, Kang X, Qin X,
548 Sun J, Li Y, Jiang X (2014) Integrated microcapillary for sample-to-answer
549 nucleic acid pretreatment, amplification, and detection. *Anal Chem* 86:10461-
550 10466.

551 (14) Chen F, Zhao Y, Fan C, Zhao, Y (2015) Mismatch Extension of DNA
552 Polymerases and High-Accuracy Single Nucleotide Polymorphism Diagnostics
553 by Gold Nanoparticle-Improved Isothermal Amplification. *Anal Chem* 87:8718-
554 8723.

555 (15) Li J, Macdonald J (2015) Advances in isothermal amplification: novel
556 strategies inspired by biological processes. *Biosens Bioelectron* 64:196-211.

557 (16) Santiago-Felipe S, Tortajada-Genaro LA, Morais S, Puchades R,
558 Maquieira A (2014) One-pot isothermal DNA amplification–Hybridisation and
559 detection by a disc-based method. *Sens Actuator B-Chem* 204:273-281.

560 (17) Santiago-Felipe, S., Tortajada-Genaro, L. A., Puchades, R., Maquieira,
561 Á. (2016) Parallel solid-phase isothermal amplification and detection of multiple
562 DNA targets in microliter-sized wells of a digital versatile disc. *Microchimica*
563 *Acta*, 183:1195-1202.

564 (18) Tortajada-Genaro LA, Santiago-Felipe S, Amasia M, Russom A,
565 Maquieira A (2015) Isothermal solid-phase recombinase polymerase
566 amplification on microfluidic digital versatile discs (DVDs). *RSC Adv* 5:29987-
567 29995.

568 (19) Li Z, Liu Y, Wei Q, Liu Y, Liu W, Zhang X, Yu Y (2016) Picoliter Well
569 Array Chip-Based Digital Recombinase Polymerase Amplification for Absolute
570 Quantification of Nucleic Acids. *PLoS one*, 11:e0153359.

571 (20) Daher RK, Stewart G, Boissinot M, Boudreau DK, Bergeron MG (2015)
572 Influence of sequence mismatches on the specificity of recombinase
573 polymerase amplification technology. *Mol Cell Probes* 29:116-121.

574 (21) Shin Y, Perera AP, Kim KW, Park MK (2013) Real-time, label-free
575 isothermal solid-phase amplification/detection (ISAD) device for rapid detection
576 of genetic alteration in cancers. *Lab Chip* 13:2106-2114.

577 (22) NgePN, Rogers CI, Woolley AT (2013) Advances in microfluidic
578 materials, functions, integration, and applications. *Chem Rev* 113:2550-2583.

579 (23) Bhattacharjee N, Urrios A, Kang S, Folch A (2016) The upcoming 3D-
580 printing revolution in microfluidics. *Lab Chip* 16:1720-1742.

581 (24) Waheed S, Cabot JM, Macdonald NP, Lewis T, Guijt RM, Paull B,
582 Breadmore MC (2016) 3D printed microfluidic devices: enablers and barriers.
583 *Lab Chip* 16:1993-2013.

584 (25) Bierut LJ, Madden PA, Breslau N, Johnson EO, Hatsukami D, Pomerleau
585 OF, Swan GE, Rutter J, Bertelsen S, Fox L, Fugman D, Goate AM, Hinrichs AL,
586 Konvicka K, Martin NG, Montgomery GW, Saccone NL, Saccone SF, Wang JC,
587 Chase GA, Rice JP, Ballinger DG (2007) Novel genes identified in a high-density
588 genome wide association study for nicotine dependence. *Hum Mol Gen* 16:24-
589 35.

590 (26) Carpenter MJ, Jardin BF, Burris JL, Mathew AR, Schnoll RA, Rigotti NA,
591 Cummings KM (2013) Clinical strategies to enhance the efficacy of nicotine
592 replacement therapy for smoking cessation: a review of the literature. *Drugs*,
593 73:407-426.

594 (27) Moody C, Newell H, Viljoen H (2016) FA mathematical model of
595 recombinase polymerase amplification under continuously stirred conditions.
596 *Biochem Eng J* 112:193-201.

597 (28) Dimitrov RA, Zuker M (2004) Prediction of hybridization and melting for
598 double-stranded nucleic acids. *Biophys J* 87:215-226.

599 (29) Zhang C, Xing D (2007) Miniaturized PCR chips for nucleic acid
600 amplification and analysis: latest advances and future trends. *Nucleic Acids Res*
601 35:4223-4237.

602 (30) Liu B, Huang PJJ, Zhang X, Wang F, Pautler R, IpACF, Liu J (2013)
603 Parts-per-million of polyethylene glycol as a non-interfering blocking agent for
604 homogeneous biosensor development. *Anal Chem* 85:10045-10050.

605 (31) Wu J, Kodzius R, Cao W, Wen W (2014) Extraction, amplification and
606 detection of DNA in microfluidic chip-based assays. *Microchim Acta* 181:1611-
607 1631.

608 (32) Li J, Wang L, Mamon H, Kulke MH, Berbeco R, Makrigiorgos GM (2008)
609 Replacing PCR with COLD-PCR enriches variant DNA sequences and
610 redefines the sensitivity of genetic testing. *Nat Med* 14:579–84.

611 (33) Shen R, Fan JB, Campbell D, Chang W, Chen, J., Doucet, D., Yeakley J,
612 Bibikova M, Garcia EW, McBride C, Steemers F, Garcia F, Kermani BG,
613 Gunderson K, Oliphant A (2005) High-throughput SNP genotyping on universal
614 bead arrays. *Mut Res Fund Mol M* 573:70-82.

615 (34) David SP, Strong DR, Leventhal AM, Lancaster MA, McGearry JE,
616 Munafò MR, Bergen AW, Swan GE, Benowitz NL, Tyndale RF, Conti DV,
617 Brown RA, Lerman C, Niaura R (2013) Influence of a dopamine pathway
618 additive genetic efficacy score on smoking cessation: results from two
619 randomized clinical trials of bupropion. *Addiction* 108:2202-2211.

620